31st Annual International Conference of the IEEE EMBS
Minneapolis, Minnesota, USA, September 2-6, 2009

A Computer Study of the Effects of Branching Dimension on Safety Factor Distribution and Propagation in a Cardiac Conduction Network

Jichao Zhao,[1] Bruce H Smaill,[1,2] and Andrew J Pullan[1,3]

Abstract— **Branching conduction networks are responsible for coordinated distribution of activation throughout the heart, but the effects of branching geometry on the efficiency of distribution and the safety of propagation remain unclear. We have developed a simplified computer model to investigate this issue in a systemic fashion. A simplified 2D model that reproduces key features of the right atrial pectinate muscle network has been developed. This consists of a large main strand that gives rise to regularly spaced perpendicular branches. Safety factor (SF) and activation time (AT) within the network are estimated for a range of different branch dimensions. The SF is reduced as branch dimension is increased due to the larger current load and is least at the proximal edge of the junction between the main strand and branches. On the other hand, activation efficiency depends on appropriate balance between the load imposed by branching and source which they subsequently provide. With repeated stimulation at progressively decreasing coupling intervals, the SF and conduction fall within the network, but the locations of block varied with branching dimension, again reflecting spatial variation in the balance between current source and current load. We hypothesize that the observed geometry of the branching network optimizes distribution efficiency and propagation safety.**

I. INTRODUCTION

Experimental and computational studies [1], [4] have shown that regular branching of conduction pathways in the atrioventricular (AV) node contributes to robust, slow conduction through that structure. Kucera and Rudy (2001) [5] investigated the effects of regular side branches along a 1D tract of ventricular cells represented by the Luo-Rudy dynamic model. They demonstrated that branching delayed conduction, but did so with relatively little loss of propagation safety overall because activated branches provided a current source for downstream excitation. Their analysis dealt specifically with a 1D structure in which side branches were terminated. However, branching quasi-2D networks such as the Purkinje fiber system and the pectinate muscles (PM) are responsible for coordinated distribution of activation throughout the cardiac chambers [1], [6], [7], [17]. The effects of branching geometry on the efficiency of distribution and safety of propagation in such networks have not been investigated.

In this study, we seek to develop a simplified 2D model that captures key features of network geometry based on a pig right atrial appendage (RAA), but will enable such features as branch dimension, and potentially frequency of branching, to be varied in a systematic fashion.

This work is supported by Health Research Council of New Zealand.

[1]Bioengineering Institute, The University of Auckland, 1142, New Zealand, j.zhao@auckland.ac.nz

[2]Department of Physiology, The University of Auckland, 1142, New Zealand, b.smaill@auckland.ac.nz

[3]Department of Engineering Science, The University of Auckland, 1142, New Zealand, a.pullan@auckland.ac.nz

II. METHODS

The 3D structure of the pig RAA is complex [8], [9], with a hierarchy of interconnected subendocardial muscle branches (mainly the crista terminalis (CT) and PM) that interface with the relatively thin layer of atrial myocytes which constitute the smooth outer wall of the atria (see Fig. 1A). Similar branch structures exist in the endocardial surfaces of the left atrium. For the pig RAA studied, the maximum diameter of the CT is 6.30 mm, while the mean diameter of the PM branches varies dramatically from 0.25 to 3.01 mm. Conduction velocity in these branches is around 1.2∼1.7 m/s, while it reduces to around 0.7 m/s in the atrial wall [9]. While branching networks are associated with conduction delay, the impact of the size variation in PM branches remains unclear. It is difficult to use structurally detailed anatomic models to investigate this issue (see Fig. 1B). Therefore, we have developed a simplified model that allows to address the effects of branch size on propagation and propagation safety.

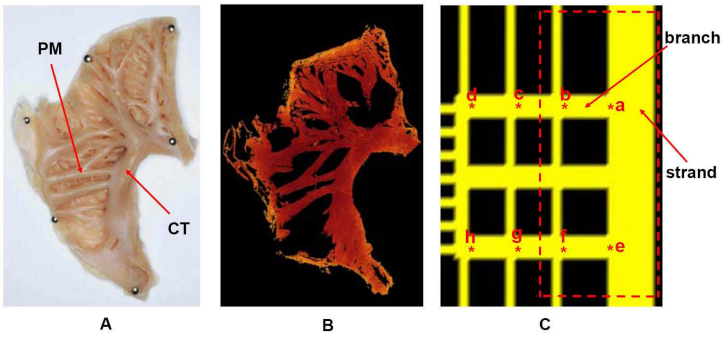

Fig. 1. A simple 2D branch network model. (A) A pig RAA tissue before wax embedding. (B) One 2D image section contains major PM branches and the CT. (C) A simplified 2D computer model based on the branch structure of the RAA. The spatial discretization steps are 0.1 mm. (a-h) are used as reference points for later results.

A. A simple 2D computer model

In our recent computer simulation work on the RAA [9], we compared 2D and 3D models, and concluded that the 2D computer model, based on realistic anatomical structure (see Fig. 1B), was sufficient to explore arrhythmogenesis. This observation was further supported by Starmer [10]. In this paper, we propose a simplified 2D computer model as

shown in Fig. 1C. The width of the thick vertical strand is about 1 mm, which is used to mimic the CT bundle. The three horizontal branches are simplified versions of the PM bundles (the width shown in Fig. 1C is 0.5 mm). Other smaller branches with the width 0.2 mm are used to connect to other current load (not shown in Fig. 1C) to mimic the presence of the atrial free wall. In our numerical experiments, we use 0.3, 0.5 and 0.7 mm respectively for the size of the PM branches while the size of the CT remains fixed at 1 mm. The Courtemanche et al. [12] human atrial activation cell model was used in our computer simulations.

A regular orthogonal finite element mesh was constructed, and preconditioned conjugate gradient methods were used to solve the bidomain equations. Then an operator splitting scheme was employed to advance the reaction diffusion equation of the bidomain formulation implicitly in the time and a forward Euler integrator was chosen to solve for membrance currents. To quantitively measure the impact of varying branch width on slow conduction, we compare activation time and the SF. It is quite straightforward to compute activation time at every grid node using the bidomain model. In the following section, we will discuss how to compute the SF.

B. Safety factor computation

The SF is used to measure the success of propagation at each cell (grid node) and is the ratio of the total charge produced to the total charge consumed at that cell. If the ratio is less than 1, inefficient charge is produced for downstream activation, propagation will fail.

Shaw and Rudy [13] computed the SF for the 1D problem as follows

$$\mathrm{SF} = \frac{Q_{\mathrm{out}} + Q_{\mathrm{c}}}{Q_{\mathrm{in}}} \qquad (1)$$

The total charge consumed Q_{in} in the equation 1 is computed by integrating over a time interval **A** of current entering the cell. Here, we chose the lower and upper bound of the time interval **A** as the instant when the membrane potential derivative reaches 1% of its maximum and the instant when membrane potential is maximal respectively. This choice has the advantages of simplicity and robustness [14], [15], [16]. The term Q_{out} in the numerator of the equation 1, total charge passed to neighbors Q_{out}, can be computed similarly by integrating current exiting the cell over the same time integral **A**. The capacitive charge of the membrane Q_{c}, the energy reserved for the membrane repolarization, is equal to the time integral of the membrane capacitive current. The 2D or 3D SF can be calculated in a similar way.

III. Results

A. A safety factor distribution and activation time

Using the method outlined in section II-B, we computed the 2D SF at the junctions of the strand and branches (the area inside the dotted rectangle shown in Fig. 1C). A stimulus was applied to a row of three grid points at the right top

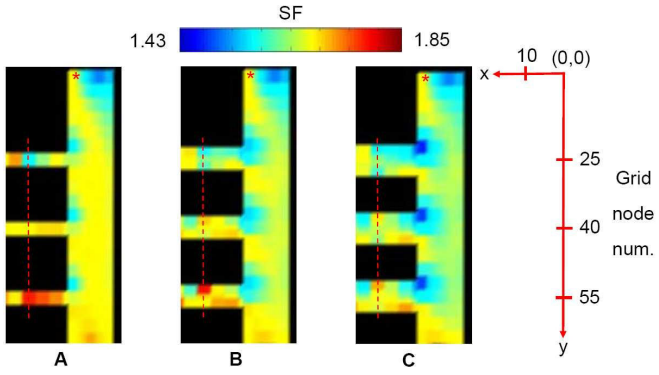

Fig. 2. The effects of branch dimension on the safety factor (SF) distribution. The computed SF is distributed in the branching areas of the strand (width 1 mm) with branch width 0.3, 0.5, and 0.7 mm in (A), (B) and (C), respectively. Red stars indicate where the origin of the coordinate system (x, y) is located, which is used for displaying values of the SF later on.

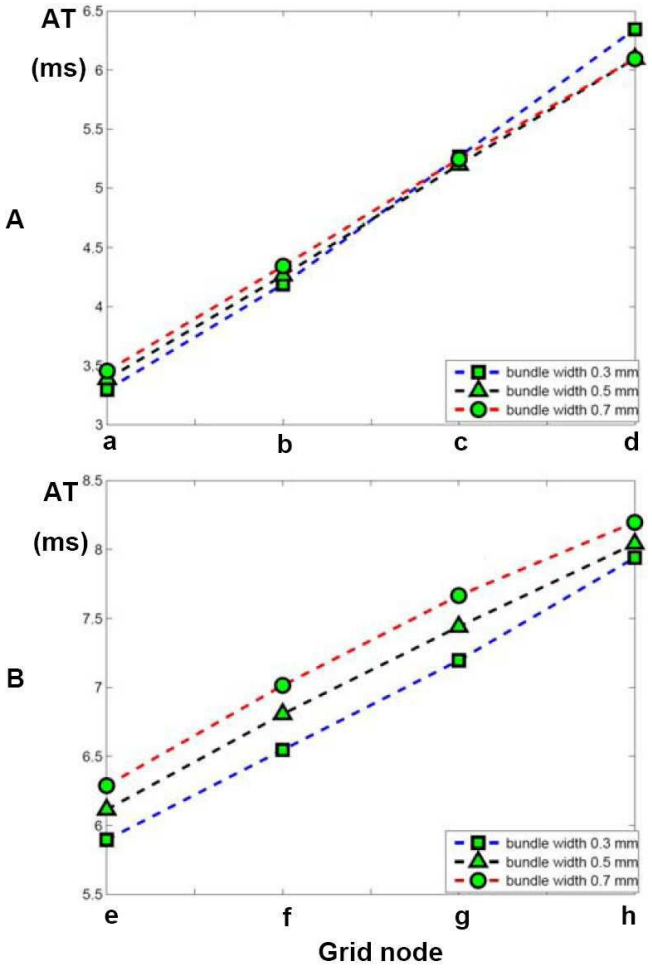

Fig. 3. The effects of branch dimension on activation time (AT) at sites indicated in Fig. 1C. (A) AT for selected grid nodes (a-d) in the first PM branch. (B) AT for selected grid nodes (e-h) in the third branch.

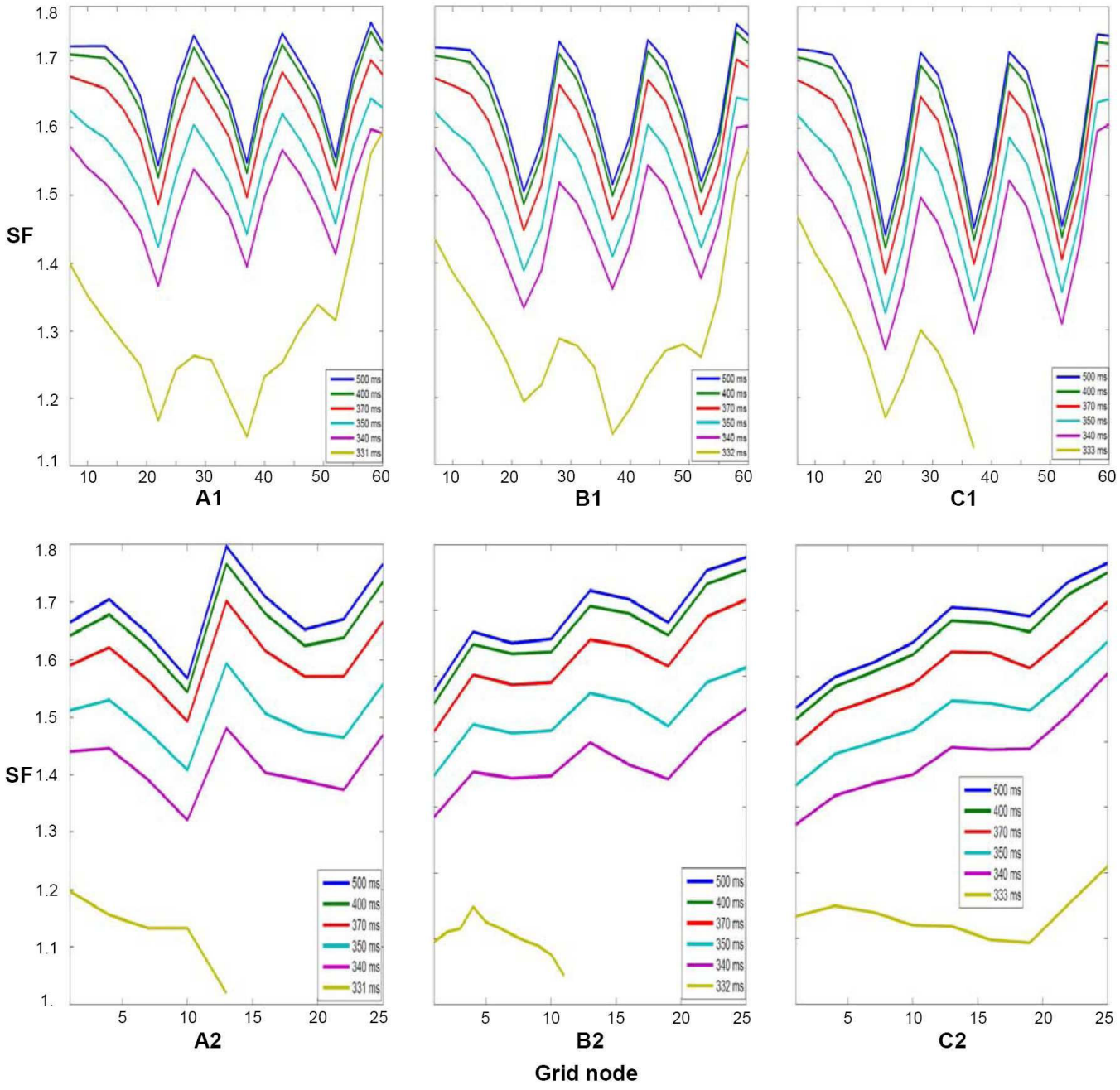

Fig. 4. Safety factor (SF) distributions for a pair of stimuli S1-S2 with progressively reduced coupling interval (CI) for branch widths of 0.3, 0.5 and 0.7 mm (A, B and C). The variation of the SF along the strand (the y-axis direction in Fig. 1C) and the central line of the first PM branch (the x-axis direction in Fig. 1C) is presented in upper and lower panels, respectively. Grid locations for both are shown in Fig. 2C where the site of the origin is also indicated by the red star. The SF distributions at representative CIs are colour coded.

corner of the main strand (Fig. 1C). Fig. 2(A,B,C) displays the computed SF distributions for branch widths of 0.3, 0.5 and 0.7 mm respectively. The SF is reduced progressively as branch dimensions are increased, presumably as a result of increased current load. This is most marked immediately upstream of the branch junctions, but there are also more subtle variations in the SF across the three PM branches due to internal current loading within the network.

The effects of branch dimension on propagation delays are more subtle (Fig. 3). Activation delays along the main strand lengthen progressively as branch dimensions increase (refer to sites **a** and **e** in Fig. 3), because current loading is increased. On the other hand, activation delays along the branches are reduced as branch dimensions increase (Fig 3A), because the current source available to activate the remaining networks is increased. Overall distribution delays are minimized between 0.3 and 0.5 mm.

B. Conduction block and stimulus coupling interval

There is compelling experimental [11] and theoretical [9] evidence that conduction block can occur at the junction of the CT and PM branches in the RAA and it is thought that this may contribute to initiation and maintenance of atrial arrhythmias. We have estimated the SF distributions during the application of stimulus pair S1-S2 to the same area as the previous section in which the coupling interval (CI) between the two stimuli is progressively reduced until conduction failure occurs.

In Fig. 4, we presented the SF distributions along the strand (upper panel) and along the central line of the first PM branch (lower panel) for reducing CI, for branch width of 0.3, 0.5 and 0.7 mm (A, B and C, respectively). With a branch width of 0.7 mm, conduction block occurs first in the CT adjacent to the second PM branch (the break point in the yellow line of the Fig. 4C1). However, for branch widths of 0.3 and 0.5 mm, conduction fails within the first PM branch (the break points in the yellow lines of the Fig. 4A2, 4B2). In all cases, block occurs at CI $\sim$330 ms. We interpret the differing locations of conduction failure within the network for different branch dimensions as being due to altered source/load balance as discussed previously. It is noteworthy that the SF is reduced progressively as CI is reduced, but falls sharply as conditions for conduction failure are approached.

IV. Conclusion

Using our simple 2D model, it has been possible to investigate the effects of geometry on activation efficiency and propagation safety in a branching conduction network. Our findings are summarized below.

1) The SF is reduced within the strand and in the branches adjacent to it as branch size increases.
2) The SF is least at the interface between the strand and branches in regions proximal to the stimulus site.
3) Activation efficiency is optimized when relative strand and branch dimensions ensure that current source/load balance is maintained throughout the network.
4) With the S1-S2 stimuli at progressively reducing CI both the SF and conduction velocity decrease with CI. In general, conduction failure occurs in regions where the SF is least under normal circumstances, but the precise location is affected by rate dependent regional current source/load balance.

We hypothesize that the geometry of branching conduction networks is consistent with optimal distributional efficiency and propagation safety.

V. Acknowledgments

This work is funded by Health Research Council of New Zealand. The first author would like to acknowledge the very helpful discussion with Prof. Wim Lammers.

References

[1] Kleber AG, and Rudy Y. Basic mechanisms of cardiac impulse propagation and associated arrhythmias. Physiol Rev 2004; 84: 431-488.
[2] Rohr S, Kucera JP, Klber AG. Slow conduction in cardiac tissue, I: effects of a reduction of excitability versus a reduction of electrical coupling on microconduction. Circ Res. 1998;83:781-794.
[3] Rohr S. Role of gap junctions in the propagation of the cardiac action potential. Cardiovascular Research 2004;62:309-322.
[4] Meijler FL, Jalife J. AV node function during atrial fibrillation. In: Mazgalev TN, Tchou PJ, eds. Atrial-AV Nodal Electrophysiology: A View From the Millenium. Armonk, NY: Futura Publishing Company; 2000: 251-268.
[5] Kucera JP, and Rudy Y. Mechanistic insights into very slow conduction in branching cardiac tissue: a model study. Circulation Research 2001;89:799.
[6] Spach MS, Miller WT, Dolber PC, Kootsey JM, Sommer JR, Mosher CE: The functional role of the structural complexities in the propagation of depolarization in the atrium of the dog: cardiac conduction disturvances due to discontinuities of effective axial resistivity. Circ Res 1982; 50:175-191.
[7] Kucera JP, Klber AG, Rohr S. Slow conduction in cardiac tissue, II: effects of branching tissue geometry. Circ Res. 1998;83:795- 805.
[8] Sands GB, Gerneke, Smaill, and Legrice. Automated extended volume imaging of tissue using confocal and optical microscopy. 28th Annual International Conference of the IEEE 2006.133-136.
[9] Zhao J, Trew ML, Legrice IJ, Smaill BH, and Pullan AJ. A tissue-specific model of reentry in the right atrial appendage. Journal of Cardiovascular Electrophysiology 2009;20(6): 675-684.
[10] Starmer CF. Exploring reentrant arrhythmias with numerical experiments: generic properties and model complexity. Journal of Cardiovascular Electrophysiology 2009;20(6): 685-688.
[11] Becker RB, Bauer A, Metz S, Kinscherf R, Senges JC, Schreiner KD, Voss F, Kuebler W, Schoels W: Intercaval block in normal canine hearts: role of the terminal crest. Circ Res 2001; 103:2521-2526.
[12] Courtemanche M, Ramirez RJ, Nattel S: Ionic mechanisms underlying human atrial action potential properties: insights from a mathematical model. Am J Physiol Heart Circ Physiol 1998; 275:301-321.
[13] Shaw RM, Rudy Y. Ionic mechanisms of propagation in cardiac tissue: roles of the sodium and L-type calcium currents during reduced excitability and decreased gap junction coupling. Circ Res. 1997;81:727-741.
[14] Azene EM, Trayanova NA, Warman E. Wave front-obstacle interactions in cardiac tissue: a computational study. Ann Biomed Eng. 2001;29: 35-46.
[15] Romero L, Trenor B, Ferrero JM, and Saiz J. A sensitivity study of the safety factor for conduction in the myocardium. Computers in Cardiology 2005;32: 873-876.
[16] Romero L, Trenor B, Ferrero JM, Saiz J, Molt G, and Alonso JM. Safety factor in simulated 2D cardiac tissue: influence of altered membrane excitability. Computers in Cardiology 2006;33: 217-220.
[17] Takebayashi-Suzuki K, Yanagisawa M, Gourdie RG, Kanzawa N and Mikawa T. In vivo induction of cardiac Purkinje fiber differentiation by coexpression of preproendothelin-1 and endothelin converting enzyme-1. Development, The Company of Biologists Limited, Great Britain, 2000;127: 3523-3532.